GEOPHYSICS, VOL. 70, NO. 1 (JANUARY-FEBRUARY 2005); P. T1–T11, 6 FIGS.
10.1190/1.1852788

Radiative transfer in layered media and its connection to the O'Doherty-Anstey formula

Matthew M. Haney[1], Kasper van Wijk[2], and Roel Snieder[1]

ABSTRACT

We examine radiative transfer theory, which accounts for the multiple scattering of waves, in a layered medium composed of randomly placed thin beds excited by a 1D source. At its most basic level, radiative transfer predicts that the wavefield separates into a coherent, or wavelike, part and an incoherent, or diffusive, flow after a length scale known as a mean free path. The dynamic properties of the coherent and incoherent wavefield are linked. For 1D Rayleigh scatterers, or thin beds, we show that the exponential decay of the coherent wave predicted by radiative transfer corresponds to the decay predicted by the O'Doherty–Anstey formula. This equivalence reveals an underlying relationship between radiative transfer and mean field theory. Finite-difference simulations of the scalar wave equation with randomly placed thin beds demonstrate the diffusive behavior of the incoherent energy at late times.

INTRODUCTION

The subsurface is disordered at any length scale, including the scale of seismic wavelengths. We consider the type of random medium depicted in Figure 1: a series of layers embedded in a constant-velocity background that are thin compared to the dominant wavelength and are of varying reflection strength. Describing wave propagation in this setting requires the inclusion of thin-bed effects. O'Doherty and Anstey (1970) state that the amplitude of a wave transmitted through a stack of thin layers decays exponentially with distance as

$$|T| \sim \exp(-\tilde{R}(k)z), \tag{1}$$

where $\tilde{R}(k)$ represents the power spectrum of the average reflection coefficient series normalized by two-way travel distance (Banik et al., 1985; Shapiro and Zien, 1993). The fundamental physics that emerges from equation 1 is the stratigraphic filtering that a wave undergoes as it propagates through thin layers. This filtering action is rooted in the phenomenon of multiple wave scattering: the amplitude of a wave transmitted through a stack of thin layers is much larger than can be expected by considering only the direct, purely forward-scattered wave. Hence, multiple scattering defines the amplitude of waves transmitted through thin layering.

Equation 1 is commonly referred to as the O'Doherty–Anstey formula and has subsequently been derived from a statistical point of view, or mean field theory (Banik et al., 1985), from a deterministic approach (Resnick et al., 1986), and via the concept of self-averaging quantities (Shapiro and Hubral, 1999). The method we present falls into the statistical category: we verify the O'Doherty–Anstey formula by studying the second statistical moment of the average wavefield, or average intensity, instead of the first statistical moment, or mean field. The theory for the spatial and temporal evolution of a wavefield's average intensity is known as radiative transfer (Chandrasekhar, 1960). It has its origins in the kinetic theory of gases and is sometimes referred to as Boltzmann transport theory (Saaty, 1981, p. 321) in honor of its earliest proponent. In the earth sciences, it first appeared within the context of light propagation through the atmosphere (Schuster, 1905). Since the 1980s, geophysicists have begin to investigate multiply scattered seismic waves using the theory of radiative transfer (Wu and Aki, 1988; Wu, 1993, 1998; Wu and Xie, 1994; Sato and Fehler, 1998; Margerin et al., 1999). The theory has several strengths; for instance, using radiative transfer, scattering attenuation and intrinsic absorption can be estimated individually (Wu and Aki, 1988; Wu, 1998; van Wijk et al., 2004).

We derive results from radiative transfer that agree with results from mean field theory (Banik et al., 1985), namely, the O'Doherty–Anstey formula. Such an equivalence suggests that radiative transfer is a proper extension of mean field theory (a variance field theory) for the fluctuating, multiply scattered waves in this regime. We note that, following Shapiro

Manuscript received by the Editor April 16, 2003; revised manuscript received June 21, 2004; published online January 14, 2005.
[1]Colorado School of Mines, Center for Wave Phenomena, Golden, Colorado 80401. E-mail: mhaney@dix.mines.edu; rsnieder@mines.edu.
[2]Colorado School of Mines, Physical Acoustics Laboratory, Golden, Colorado 80401. E-mail: kasper@acoustics.mines.edu.

and Hubral (1999), mean field theory and the O'Doherty–Anstey formula coincide only for low frequencies. In addition, we show that at late times the equation of radiative transfer can be simplified to the diffusion equation. This agrees with the observation that the individual solutions to these equations match at late times (Sheng, 1995; Ishimaru, 1997; Paasschens, 1997; Scales and van Wijk, 2001). Results of finite-difference simulations of the 1D scalar wave equation with random thin beds are presented to support the accuracy of this approximation. After estimating the two parameters needed to describe energy transport—the group velocity and mean free path—we find that the average intensity of the numerical simulations approaches the diffusive limit with time. Our results complement previous numerical experiments in 1D random media by Wu and Xie (1994) that examined the stationary (time-integrated) problem. By additionally looking at the temporal behavior, we gain more insight into the applicability and limitations of radiative transfer in one dimension.

As a result of interference phenomena in the presence of thin beds, or interbed multiples, radiative transfer is, strictly speaking, not completely valid in describing energy transport in randomly layered media (Papanicolaou, 1998). We address this shortcoming of radiative transfer when discussing our numerical results. Though critical in one dimension, these same interference phenomena become much less important in the presence of higher dimensional disorder (e.g., 3D disorder), making radiative transfer the theory of choice when studying, for instance, the coda of earthquakes (Hennino et al., 2001). The fact that interference dominates in one dimension has effectively kept the terminology of radiative transfer out of the study of randomly layered structures. But before discarding such a theory, we demonstrate that radiative transfer, despite these reservations, has more applicability in one dimension than has been believed.

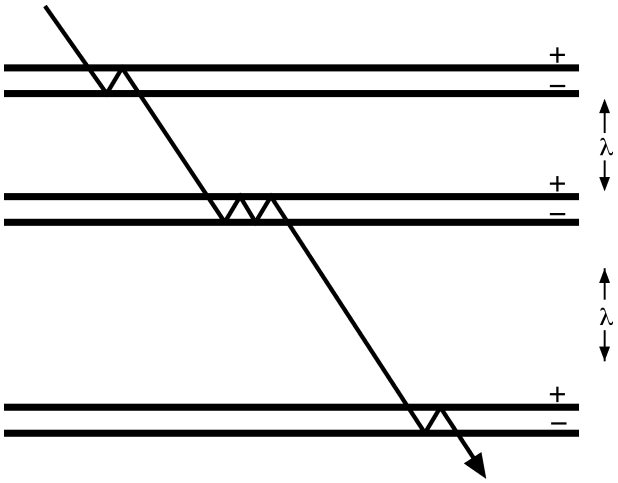

Figure 1. The model considered in this paper: a wave transmitted through a random sequence of thin beds that are separated by more than one wavelength. The thin beds are embedded in a constant-velocity background medium and may themselves have varying reflection coefficients. Adapted from O'Doherty and Anstey (1970).

RADIATIVE TRANSFER THEORY

The radiative transfer equation can be derived from energy balance considerations (Morse and Feshbach, 1953; Chandrasekhar, 1960; Turner, 1994; Ishimaru, 1997). Heuristically, the equation takes the form

$$[\partial_t + v \cdot \nabla]\,\text{intensity} = \text{source} - \text{loss} + \text{gain}. \quad (2)$$

The left-hand side of equation 2 is the total time derivative of the intensity. On the right-hand side, loss and gain mechanisms in addition to sources determine the dynamic behavior. In the absence of loss or gain, this equation becomes the one-way wave equation. Scattering and absorption show up as loss mechanisms since both remove energy from the forward direction. Only scattering can put energy back into the original direction of propagation. Hence, scattering and absorption enter equation 2 in fundamentally different ways: scattering enters the gain term while the loss term contains both scattering and attenuation. This fact leads to the possibility of separating their effects with radiative transfer theory.

By squaring a wavefield and averaging over many realizations of a random medium, we lose the phase information of the underlying wavefield. What remains is the average intensity, or squared amplitude—the quantity appearing on the left-hand side of equation 2. The advantages of studying the spatial and temporal evolution of the intensity via radiative transfer lie in the ability to gain statistical information about the structure of a medium at scales less than a wavelength and the description of the decoupling of scattering and absorption for incoherent wave energy.

Using the same form as equation 2, we present a scalar radiative transfer equation valid for any dimension (Turner, 1994):

$$\begin{aligned}\frac{\partial I(\vec{r},\Omega,t)}{\partial t} + v\hat{n}(\Omega)\cdot\nabla I(\vec{r},\Omega,t) &= S(\vec{r},\Omega,t)\\ &- \frac{1}{\tau_s}I(\vec{r},\Omega,t) - \frac{1}{\tau_a}I(\vec{r},\Omega,t)\\ &+ \frac{1}{\tau_s}\int \frac{1}{\sigma_s}\frac{\partial\sigma_s}{\partial\Omega'}I(\vec{r},\Omega',t)\,d\Omega', \end{aligned} \quad (3)$$

where $I(\vec{r},\Omega,t)$ is the intensity, or average squared wavefield, at position $\vec{r}$ and time t propagating in direction Ω, v is the group velocity of the average (coherent) wavefield, $\hat{n}$ is the unit vector in the direction of propagation, and $S(\vec{r},\Omega,t)$ is the angle-dependent source function. The differential scattering cross-section $\partial\sigma_s/\partial\Omega'$ describes the exchange of energy traveling from direction Ω into direction Ω'. The characteristic time between these exchanges is τ_s, the scattering mean free time. The total scattering cross-section σ_s is a measure of the energy exchanged in all directions:

$$\sigma_s = \int \frac{\partial\sigma_s}{\partial\Omega'}d\Omega'. \quad (4)$$

Intrinsic attenuation is included via the characteristic absorption time τ_a.

Using terminology originally coined by Clausius in the 1800s (Lindley, 2001, p. 25), it is common to define mean free paths for scattering and absorption, ℓ_s and ℓ_a, according to the relations $\ell_s = v\tau_s$ and $\ell_a = v\tau_a$. The scattering mean free path

ℓ_s can be thought of as the typical distance a wave travels between scattering events. Both ℓ_s and ℓ_a can be related to the parameter Q more commonly used in seismology:

$$\ell_s = \frac{vQ_s}{2\pi f} \quad \text{and} \quad \ell_a = \frac{vQ_a}{2\pi f},$$

where Q_s and Q_a refer to the scattering and absorption Q, respectively, and f is the frequency.

The scattering mean free path ℓ_s is inversely proportional to the number of thin beds per unit depth (the number density) ρ and their scattering cross-section. As a reasonable approximation,

$$\ell_s = \frac{1}{\rho\sigma_s}. \tag{5}$$

This equation, called the independent scattering approximation, holds when the scatterers are weak and separated by more than a wavelength. It is one of the fundamental results from multiple scattering theory, and it also appears in the kinetic theory of gases. Equation 5 can be found in standard texts (Lax, 1951; Morse and Feshbach, 1953; Feynman et al., 1963). Certainly, more general expressions for ℓ_s exist within the field of multiple wave scattering (van Tiggelen et al., 1991); however, in the interest of simplicity, we adopt equation 5 for this paper. Note that, from equation 5, ℓ_s contains information about the product of ρ and σ_s in a way analogous to a wave reflected from an interface containing information about the acoustic impedance.

RADIATIVE TRANSFER IN LAYERED MEDIA

Since in one dimension only two directions of propagation exist (forward/backward or up/down), a general expression for the differential scattering cross-section, appearing under the integral in equation 3, is

$$\frac{\partial\sigma_s(\Omega,\Omega')}{\partial\Omega'} = E_f\delta(\Omega'-\Omega) + E_b\delta(\Omega'+\Omega-180^\circ), \tag{6}$$

where E_b and E_f represent amounts of energy back-scattered, and forward-scattered, divided by the energy of the incident wave. Hence, E_b and E_f are dimensionless. Their sum is equal to the total scattering cross-section,

$$\sigma_s = E_b + E_f. \tag{7}$$

Thus, in equation 3 the differential scattering cross-section divided by the total scattering cross-section becomes

$$\frac{1}{\sigma_s}\frac{\partial\sigma_s(\Omega,\Omega')}{\partial\Omega'} = \frac{E_f}{E_b+E_f}\delta(\Omega'-\Omega) + \frac{E_b}{E_b+E_f}\delta(\Omega'+\Omega-180^\circ). \tag{8}$$

We denote the ratios $E_f/(E_b + E_f)$ and $E_b/(E_b + E_f)$ by F and B, respectively. These ratios satisfy $B + F = 1$. In the case of isotropic scattering, $B = F = 1/2$; (Paasschens, 1997). For a general 1D scatterer, B and F can be related to the total transmission and reflection coefficients of a thin bed, T_t and R_t (Sheng, 1995):

$$B = \frac{|R_t|^2}{|R_t|^2+|T_t-1|^2} \quad \text{and} \quad F = \frac{|T_t-1|^2}{|R_t|^2+|T_t-1|^2}. \tag{9}$$

Note that a thin bed consists of two interfaces. Hence, R_t and T_t are not simple reflection and transmission coefficients; rather, they include all orders of intrabed multiples. The quantities R_t and T_t can be related to a geometric summation of the interface reflection and transmission coefficients via generalized rays (Aki and Richards, 1980).

Inserting equation 8 into equation 3, we obtain, in one dimension,

$$\frac{\partial I(z,\Omega,t)}{\partial t} + v\hat{n}(\Omega)\frac{\partial I(z,\Omega,t)}{\partial z} = \frac{B}{\tau_s}I(z,180^\circ-\Omega,t) - \frac{B}{\tau_s}I(z,\Omega,t) - \frac{1}{\tau_a}I(z,\Omega,t) + S(z,\Omega,t), \tag{10}$$

where we use $B + F = 1$. Equation 10 can be evaluated for the two possible directions in one dimension, $\Omega = 0^\circ$ and 180°. We refer to these directions as down and up, respectively. For simplicity, the total intensity propagating in direction $\Omega = 0^\circ$, $I(z, 0^\circ, t)$, is represented by I_d, $I(z, 180^\circ, t)$ is represented by I_u, and the source function S is split into S_d and S_u. The coordinate system is defined such that $\hat{n}(0^\circ) = 1$ and $\hat{n}(180^\circ) = -1$. The two equations that describe the propagation of downgoing and upgoing intensities are

$$\frac{\partial I_d}{\partial t} + v\frac{\partial I_d}{\partial z} = \frac{B}{\tau_s}(I_u - I_d) - \frac{I_d}{\tau_a} + S_d, \tag{11}$$

$$\frac{\partial I_u}{\partial t} - v\frac{\partial I_u}{\partial z} = \frac{B}{\tau_s}(I_d - I_u) - \frac{I_u}{\tau_a} + S_u. \tag{12}$$

This system of partial differential equations comprises radiative transfer in one dimension and has been derived by other methods (Goedecke, 1977). In Appendix A, the system of partial differential equations is solved for both I_d and I_u. However, we choose to study the total intensity, $I_t = I_d + I_u$, since this is most easily measured in practice. The Green's function for the total intensity I_t can be expressed for $B \in [0,1]$ as

$$I_t(z,t) = \frac{1}{2}\exp\left(-\frac{Bvt}{\ell_s} - \frac{vt}{\ell_a}\right)\left[(1-c)\delta(vt+z) + (1+c)\delta(vt-z) + \frac{B}{\ell_s}H(vt-|z|) \times \left[I_0\left(\frac{B}{\ell_s}\sqrt{v^2t^2-z^2}\right) + \frac{vt+cz}{\sqrt{v^2t^2-z^2}} \times I_1\left(\frac{B}{\ell_s}\sqrt{v^2t^2-z^2}\right)\right]\right], \tag{13}$$

where I_0 and I_1 are the modified Bessel functions of the zeroth and first orders and H is the Heaviside step function. The parameter c varies the source function from upgoing ($c = -1$) to isotropic ($c = 0$) to downgoing ($c = 1$) and any combination in between (see equation A-5 in Appendix A for a formal definition of c). In equation 13, we place the source at the origin

of the coordinate system. A previous solution to 1D radiative transfer obtained by Hemmer (1961) follows from equation 13 for the case of an isotropic source ($c = 0$) and isotropic scattering, $B = 1/2$. A result identical to that of Hemmer can also be found in work by Sato and Fehler (1998).

The Green's function for the total intensity can be divided into two parts. The terms containing the δ-function propagate like a wave and are called the coherent intensity. The rest of the total intensity is referred to as the incoherent intensity. It does not propagate ballistically and, as illustrated later, at late times it propagates diffusively. Also, in Appendix A we show that each Bessel function represents a different direction of propagation for the incoherent energy.

From equation 13 we find that the decay of coherent intensity as a result of scattering, described by the first exponential term, varies with distance vt by the factor ℓ_s/B and not ℓ_s. The fact that the length scale of the exponential decay is ℓ_s/B instead of ℓ_s is unique to one dimension (Paasschens, 1997).

COHERENT INTENSITY AND THE O'DOHERTY-ANSTEY FORMULA

From the solution for the total intensity, equation 13, we know radiative transfer predicts an exponential decay from scattering for the transmitted, or coherent, wave:

$$|T| \sim \exp(-Bz/2\ell_s), \tag{14}$$

where the distance z replaces vt in equation 13 since the δ-function is nonzero only at $z = \pm vt$. The factor of 1/2 in the exponent of equation 13 shows up since radiative transfer predicts decay of the transmitted intensity—the square of the transmission coefficient. We investigate the equivalence of the exponential decay predicted by radiative transfer, equation 14, and that obtained from O'Doherty–Anstey

$$|T| \sim \exp(-\tilde{R}(k)z), \tag{15}$$

which is the same as equation 1, for the transmission of normally incident scalar waves through assemblages of weak 1D Rayleigh scatterers (thin beds). Comparing equations 14 and 15, we see that the two theories are equivalent if

$$\tilde{R}(k) = \frac{B}{2\ell_s}. \tag{16}$$

The reflection coefficient series $RC(z)$ for a medium like that shown in Figure 1 is a series of delta functions of oscillating plus and minus signs:

$$RC(z) = \sum_{j=1}^{N} R_j \left[\delta(z - d_j) - \delta(z - h - d_j)\right], \tag{17}$$

where h is the thickness of the beds; R_j and d_j represent the reflection coefficient and location of the jth bed, respectively; and N is the number of beds. For the purposes of simplifying the derivation, we assume that h is the same for all the thin beds. To calculate $\tilde{R}(k)$, we take the Fourier transform of equation 17, square its magnitude to get the power spectrum, and divide by the two-way travel distance:

$$\tilde{R}(k) = \frac{1}{2L}\left|\int_{-\infty}^{\infty} RC(z)\exp(-i2kz)dz\right|^2, \tag{18}$$

where L is the one-way travel distance, or the source–receiver distance. Note that the Fourier transform is with respect to $2k$ and not k, similar to a Born inversion formula in one-dimension (Banik et al., 1985; Shapiro and Zien, 1993; Bleistein et al., 2001).

Inserting equation 17 into equation 18 results in

$$\tilde{R}(k) = \frac{1}{2L}\left|\sum_{j=1}^{N} R_j \exp(2ikd_j)(1 - \exp(2ikh))\right|^2. \tag{19}$$

For thin layers, $kh \ll 1$ and a first-order Taylor series expansion in h leads to $1 - e^{2ikh} \approx -2ikh$. Pulling this term out of the summation yields

$$\tilde{R}(k) = \frac{4k^2h^2}{2L}\left|\sum_{j=1}^{N} R_j \exp(2ikd_j)\right|^2. \tag{20}$$

We now use a standard argument from the theory of multiple scattering: if d_j, the spacing of the thin beds, is a random variable, the crossterms in the square of the summation in equation 20 cancel in the average and the squaring can be brought inside the summation:

$$\tilde{R}(k) = \frac{2k^2h^2}{L}\sum_{j=1}^{N}\left|R_j \exp(2ikd_j)\right|^2. \tag{21}$$

Now, inside the summation the exponential does not contribute to the magnitude; therefore,

$$\tilde{R}(k) = \frac{2k^2h^2}{L}\sum_{j=1}^{N}|R_j|^2 = \frac{2k^2h^2}{L}N\langle|R_j|^2\rangle, \tag{22}$$

where $\langle|R_j|^2\rangle$ is the mean square of the interface reflection coefficients.

Returning to equation 16, to prove that radiative transfer and the O'Doherty–Anstey formula predict the same exponential decay for the transmitted wave, we set equation 22 to

$$\frac{B}{2\ell_s} = \frac{1}{L}2k^2h^2N\langle|R_j|^2\rangle. \tag{23}$$

For Rayleigh scatterers in one dimension, the radiation is isotropic (Sheng, 1995). Hence, $B = 1/2$. Rearranging equation 23,

$$\ell_s = \frac{1}{8k^2h^2\langle|R_j|^2\rangle\frac{N}{L}}. \tag{24}$$

The quantity N/L is the number density of the thin beds ρ. In the limit of weak scatterers (such that $R_j \ll 1$), $8k^2h^2\langle|R_j|^2\rangle = \sigma_s$, the scattering cross-section (see Appendix B). The presence of weak reflection coefficients is also an underlying assumption in the statistical derivation of the O'Doherty–Anstey formula from mean field considerations (Banik et al., 1985). Equation 24 can now be rewritten in a familiar form:

$$\ell_s = \frac{1}{\rho\sigma_s}. \tag{25}$$

This is recognized as equation 5, the independent scattering approximation. Previously, we stated that for this relation to hold, the scatterers (thin beds) had to be separated by at least a wavelength. Hence, in this model no reflections from below the recording depth interfere with the transmitted wave. All

of the interference resulting in the exponential decay of the direct wave originates from peg-leg multiples within the thin beds, not between them (Figure 1). Equation 25 demonstrates that, for this model, the exponential decay of the transmitted wave from the O'Doherty–Anstey formula is equivalent to that predicted by radiative transfer.

We show a conceptual diagram of this equivalence in Figure 2. From mean field theory, both the phase and the amplitude of the transmitted (coherent) wave can be obtained. However, for the incoherent energy, the mean is zero by definition. Radiative transfer can address the amplitude of the transmitted wave and the behavior of the incoherent intensity, but phase information is lost. Both theories agree in their region of overlap, as demonstrated by the case of random layering we consider here.

THE DIFFUSION APPROXIMATION

From Figure 2, one can see that the strength of radiative transfer lies in its ability to retain and describe incoherent wave energy. When attempting to separate scattering and absorption attenuation, it is critical to account for the incoherent energy (Wu and Aki, 1988; Margerin et al., 1999). In this section, we show that the equation describing the incoherent intensity becomes the diffusion equation at late times, and we solve the diffusion equation for the case of a finite random medium. Inferences on the statistical properties of the medium are often based on the late-time diffusive behavior (Boas et al., 1995)—especially in optics, where it is difficult to obtain phase information.

By subtracting equations 11 and 12 and neglecting absorption ($\tau_a \to \infty$), we obtain an expression in terms of $I_n = I_d - I_u$, the net downgoing intensity, and $I_t = I_d + I_u$, the total intensity:

$$\frac{\partial I_n}{\partial t} + \frac{2B}{\tau_s} I_n = -v \frac{\partial I_t}{\partial z}. \tag{26}$$

Similarly, by adding equations 11 and 12 and neglecting absorption ($\tau_a \to \infty$), we arrive at

$$\frac{\partial I_t}{\partial t} + v \frac{\partial I_n}{\partial z} = 0. \tag{27}$$

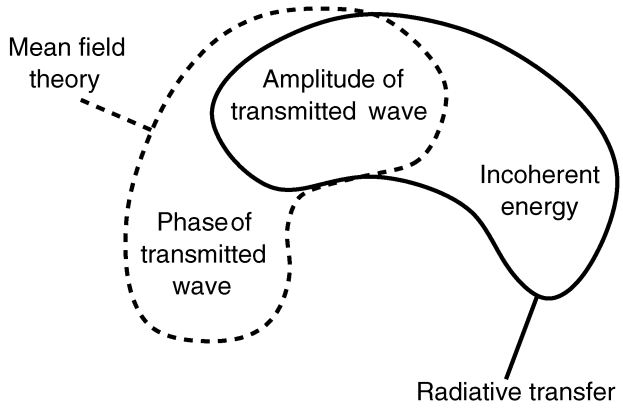

Figure 2. The overlap of O'Doherty–Anstey, which coincides with mean field theory at low frequencies (Shapiro and Hubral, 1999), and radiative transfer for the amplitude of a wave transmitted through a medium such as that depicted in Figure 1.

In the diffusive regime, the net energy flux is nearly stationary (Morse and Feshbach, 1953) and

$$\frac{2B}{\tau_s} I_n \gg \frac{\partial I_n}{\partial t}. \tag{28}$$

Under this condition, equation 26 becomes

$$\frac{2B}{\tau_s} I_n = -v \frac{\partial I_t}{\partial z}. \tag{29}$$

Substituting equation 29 into equation 27 for I_n yields

$$\frac{\partial I_t}{\partial t} + v \frac{\partial}{\partial z} \left[-\frac{\tau_s v}{2B} \frac{\partial I_t}{\partial z} \right] = 0. \tag{30}$$

Under the assumption that v and τ_s do not depend on position, equation 30 takes the form

$$\frac{\partial I_t}{\partial t} = v \left(\frac{\ell_s}{2B} \right) \frac{\partial^2 I_t}{\partial z^2}, \tag{31}$$

which we recognize as the 1D diffusion equation with the diffusion constant $D = v(\ell_s/2B)$. This implies that the movement of energy at late times has an effective mean free path that differs from ℓ_s. The effective mean free path is called the transport mean free path, $\ell_{tr} = \ell_s/2B$; hence, $D = v\ell_{tr}$. From equation 13, we stated that the length scale of the exponential decay of the coherent wave attributable to scattering also differs from ℓ_s; it is ℓ_s/B or, in terms of the transport mean free path, $2\ell_{tr}$.

To support the fact that $\ell_{tr} = \ell_s/2B$, we note that it is common (Hendrich et al., 1994) to relate ℓ_{tr} and ℓ_s via

$$\ell_{tr} = \frac{\ell_s}{1 - \langle \cos\theta \rangle}, \tag{32}$$

where $\langle \cos\theta \rangle$ represents the cosine of a direction weighted by the average scattered energy in that direction. For isotropic scattering, $\langle \cos\theta \rangle = 0$ and the two mean free paths ℓ_{tr} and ℓ_s are identical. However, using the general relation $\langle \cos\theta \rangle = F - B$ (Hendrich et al., 1994) and the fact that $F + B = 1$, equation 32 can be rewritten

$$\ell_{tr} = \frac{\ell_s}{1 - F + B} = \frac{\ell_s}{2B}, \tag{33}$$

which is exactly the relationship we derive from the diffusion approximation.

Now assume the thin beds extend over a limited depth range, from $z = 0$ to $z = L$, within an infinite homogeneous background medium (see Figure 3). For a source within the depth range of the thin beds, no intensity comes into the scattering region, i.e., the downgoing intensity is zero at $z = 0$ and the upgoing intensity is zero at $z = L$. We can express the downgoing intensity as the sum of the total intensity and the net downgoing intensity (flux) and set it to zero at $z = 0$:

$$I_d = \frac{1}{2} I_t + \frac{1}{2} I_n = 0. \tag{34}$$

Using the approximation derived in equation 29, the I_n-term can be replaced by a spatial derivative of I_t:

$$\frac{1}{2} I_t + \frac{1}{2} \left(-\frac{\ell_s}{2B} \frac{\partial I_t}{\partial z} \right) = 0. \tag{35}$$

Equation 35 can be rewritten using the definition of the transport mean free path:

$$I_t - \ell_{tr}\frac{\partial I_t}{\partial z} = 0. \tag{36}$$

This shows there is a mixed boundary condition at $z = 0$. At $z = L$, there is another boundary condition of the mixed type:

$$I_t + \ell_{tr}\frac{\partial I_t}{\partial z} = 0. \tag{37}$$

To summarize, the total intensity for a finite random medium extending from $z = 0$ to $z = L$ obeys the following boundary value problem at late times:

$$\begin{aligned}
&\frac{\partial I_t}{\partial t} = D\frac{\partial^2 I_t}{\partial z^2} + \delta(z - z')\delta(t)\\
&I_t - \ell_{tr}\frac{\partial I_t}{\partial z} = 0 \quad \text{at} \quad z = 0,\\
&I_t + \ell_{tr}\frac{\partial I_t}{\partial z} = 0 \quad \text{at} \quad z = L,
\end{aligned} \tag{38}$$

where $D = v\ell_{tr}$. Unfortunately, equation 38 cannot be solved analytically; enforcing the mixed boundary conditions leads to a transcendental equation. A well-known method to obtain a closed-form solution (Morse and Feshbach, 1953) is to transform the mixed boundary conditions into approximate Dirichlet boundary conditions:

$$\begin{aligned}
&\frac{\partial I_t}{\partial t} = D\frac{\partial^2 I_t}{\partial z^2} + \delta(z - z')\delta(t)\\
&I_t = 0 \quad \text{at} \quad z = -\ell_{tr},\\
&I_t = 0 \quad \text{at} \quad z = L + \ell_{tr}.
\end{aligned} \tag{39}$$

These approximate boundary conditions are linear extrapolations of the mixed boundary conditions in equation 38. As discussed in Morse and Feshbach (1953), the approximate boundary conditions in equation 39 work quite well, and this type of formulation is commonly used in the study of multiple wave scattering (Sheng, 1995). The approximate Dirichlet boundary conditions should not be interpreted physically; the total intensity I_t does not actually go to zero at a distance ℓ_{tr} outside the scattering region. The solution of equation 39 at the edge of the scattering region ($z = 0$ or $z = L$) holds for a receiver outside of the scattering region, with a time delay applied to allow the intensity to propagate through the homogeneous background medium to the receiver. In one dimension, equation 39 can be solved by expanding over the modes of the Laplacian,

$$I_t(z, z', t) = \frac{2}{L + 2\ell_{tr}}\sum_{m=1}^{\infty}\exp\left(-\frac{m^2\pi^2 Dt}{(L + 2\ell_{tr})^2}\right) \times \sin\left(\frac{m\pi(z + \ell_{tr})}{L + 2\ell_{tr}}\right)\sin\left(\frac{m\pi(z' + \ell_{tr})}{L + 2\ell_{tr}}\right). \tag{40}$$

The partial differential equation could have been solved equivalently by the method of images (Zauderer, 1989).

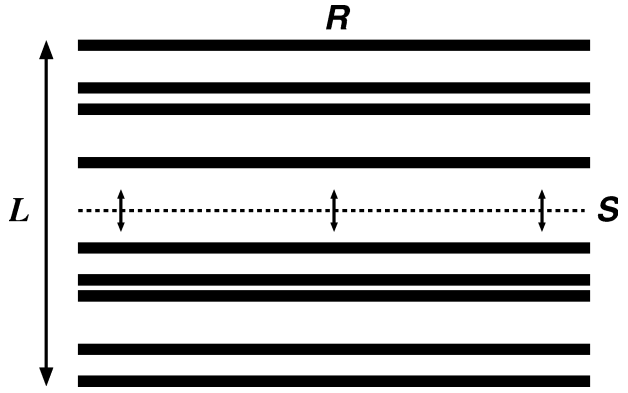

Figure 3. The geometry of the 1D numerical scattering experiments. The source is at the center of a region with thin random layers; a receiver is positioned above the layers for each experiment. The size L of the scattering region for different experiments has the values 80, 120, 160, 200, and 240 m, or, in terms of the dominant wavelength of the source, L/λ is 20, 30, 40, 50, and 60.

NUMERICAL SIMULATIONS

We tested the late-time solution 40 for the average total intensity with finite-difference simulations of the scalar wave equation in the presence of random discrete scatterers. We chose the finite-difference method since, in one dimension, perfectly absorbing boundary conditions can be applied (see Appendix C for details of the numerical implementation). This is especially important for studying the late-time behavior of a wave field when reflections from the edge of the numerical grid can overwhelm the multiply scattered waves.

The set-up of the numerical experiment is shown in Figure 3. A plane (1D) source S is excited in the center of a finite 1D random medium, of size L, containing identical but randomly spaced low-velocity (1 km/s) thin beds. By thin in this experiment, we mean their thickness is approximately one-tenth of the dominant wavelength. The high-velocity background medium in which they are embedded has a velocity of 2 km/s. We use the first derivative of a Gaussian, with a dominant wavelength of 4 m, as the source waveform. A receiver R is placed outside the scattering region. The experiment is repeated for five sizes of the scattering region, $L =$ 80, 120, 160, 200, and 240 m. We refer to these as experiments 1, 2, 3, 4, and 5, respectively. For each of the experiments, we obtain the average intensity by performing each experiment for 20 realizations of the randomness, squaring each of the 20 wavefields, and adding them.

To keep the statistical properties of the random medium the same, the number of scatterers per unit length is constant for experiments 1–5. We set the average number of scatterers per dominant wavelength to one so the independent scattering approximation holds in the simulations. The interfaces of the thin beds are in welded contact, which can be accomplished efficiently in a finite-difference scheme (Boore, 1970). Finally, we do not simulate any viscoelasticity; there is no intrinsic absorption ($\tau_a \to \infty$).

The average intensities for experiments 1–5 are plotted in Figure 4. For each of the average intensities, a high-amplitude pulse arrives first. This is the coherent intensity, or mean field. Following the coherent intensity is the incoherent multiply scattered energy. If, during the averaging process, the wavefields for the different realizations were added (stacked)

before they were squared, the incoherent energy would cancel and leave only the coherent intensity. From the moveout of the high-amplitude pulse, we find that the group velocity entering the radiative transfer equation v is approximately the velocity of the background medium (2 km/s).

To characterize the scattering in the radiative transfer model, the length scale of the exponential decay of the coherent wave, ℓ_s/B, must also be measured. The decay is depicted in Figure 5. A linear regression on a logarithmic scale estimates the characteristic distance over which the coherent wave decays exponentially. For our numerical simulations, $\ell_s/B = 46 \pm 2$ m. In the previous section, we showed that $\ell_s/B = 2\ell_{tr}$. Therefore, $\ell_{tr} = 23 \pm 1$ m. To arrive at an estimate of ℓ_s, the scattering mean free path, we would require knowledge of B, or the degree of back-scattering from an individual thin layer (van Wijk et al., 2004).

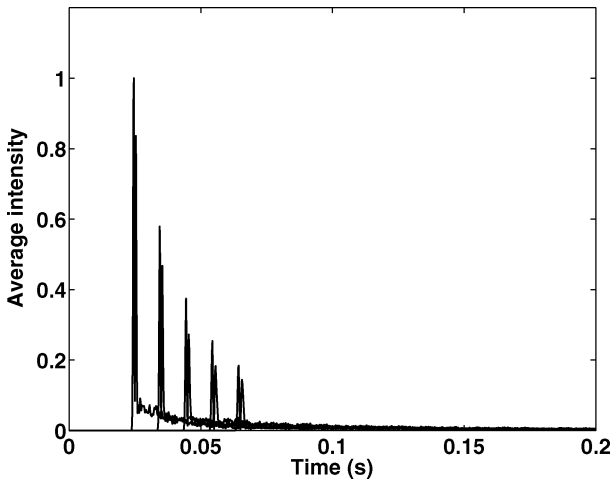

Figure 4. The average intensity measured as a function of time for the five experiments. The direct wave decays exponentially with increasing source–receiver offset because of scattering.

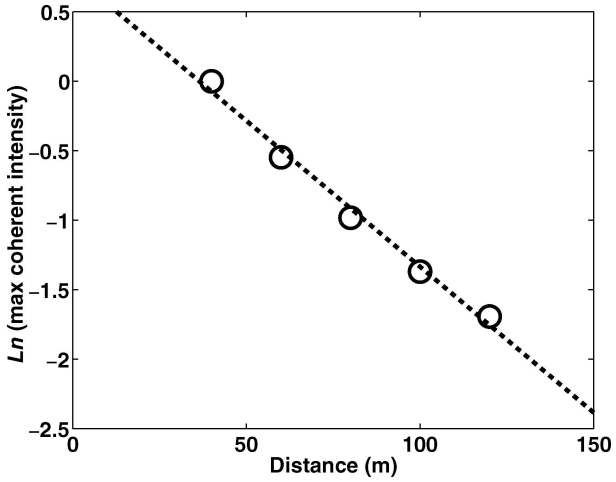

Figure 5. The maximum of the high-amplitude pulse (coherent intensity) from Figure 4 as a function of offset for experiments 1–5. A linear fit to the data in this log–linear plot gives the characteristic exponential decay caused by scattering, ℓ_s/B. We estimate $\ell_s/B = 46 \pm 2$ m.

With v and l_{tr} estimated directly from the numerical results, the theoretical prediction of equation 40 can be compared with the simulated total intensities. In Figure 6, the solution of the diffusion equation asymptotically approaches, with time, the numerical intensities of the experiment. Note that the approximation fails for early times since it is acausal. The late-time exponential decay is correctly predicted by the diffusion approximation and is largely governed by the fundamental diffusion mode ($m = 1$) in equation 40 with decay time:

$$\tau_{decay} = \frac{(L + 2\ell_{tr})^2}{\pi^2 D}. \tag{41}$$

Such behavior verifies the radiative transfer model for late times.

DISCUSSION

In higher dimensions, the radiative transfer equation becomes considerably more complicated than in one dimension since the number of directions to scatter into is infinite (Paasschens, 1997). Even in one dimension, however, the rich character of radiative transfer is evident: exponential decay of the coherent wave can be caused by both scattering and absorption, and aspects of both wave and diffusive behavior emerge in the average total intensity.

The theory of radiative transfer has its limitations, the most severe being that it does not include interference terms. For this reason, conventional wisdom is that radiative transfer is useless in the case of 1D random media (Papanicolaou, 1998). However, we have shown numerical evidence that the late-time approximation of radiative transfer, or diffusion, quantitatively describes the average intensity leaking out of a 1D randomly layered structure. These differing points of view can be reconciled. For in-situ detectors inside a 1D random

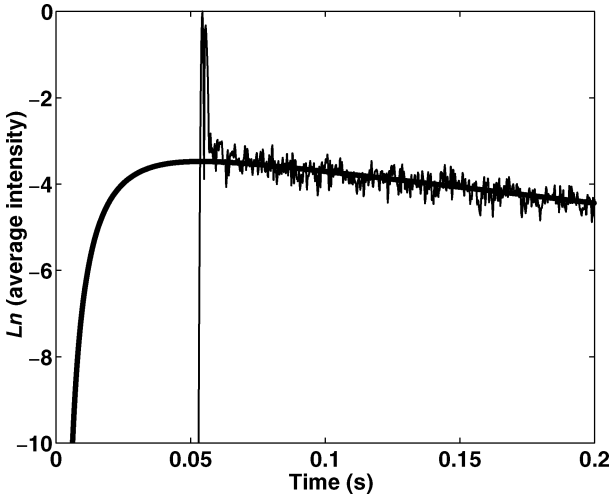

Figure 6. Logarithmic plot of the total intensity of experiment 4 (thin line) at a source–receiver offset of 100 m, compared with the diffusion approximation, equation 40. Note that the maximum of the total intensity has been normalized to unity. At early times, the analytic solution to the diffusion equation (thick line) differs from the numerical observations because the diffusion solution is acausal and does not account for the coherent field.

medium, radiative transfer and diffusion do not correctly describe the decay of the average intensity. We find agreement between our numerical experiments and radiative transfer because our receivers are always situated outside the random medium. Within the random medium, local interference, which has been studied by Spencer et al. (1982) and is not accounted for in radiative transfer, dominates the total intensity. Banik et al. (1985) discuss a way to suppress local interference since it contributes large fluctuations that can obscure the mean field behavior.

Inside a 1D random medium and at late times, the average intensity is dominated by local interference to such an extent that it does not obey diffusion (equation 40). As a function of distance from the source position, the average intensity goes down exponentially at late times instead of nonexponentially as predicted by equation 40. This behavior, inside a 1D random medium, is termed localization since the bulk of the incoherent wave field intensity is, on average, trapped locally at the source. Outside a 1D random medium, the local interference vanishes and the diffusive behavior is evident. For higher dimensional disorder, the influence of local interference is considerably less pronounced. Indeed, the observation of localization in 3D random media is disputed (Wiersma et al., 1997; Scheffold et al., 1999). Our definition of localization, describing the spatial distribution of late-time incoherent wave energy, is not the only definition of localization within the field of waves in random media (Shapiro and Hubral, 1999).

We have further demonstrated the validity of radiative transfer in layered media by linking its description of the decay experienced by the coherent wave to the O'Doherty–Anstey formula. We believe the link can be extended beyond the 1D Rayleigh-scatterer approximation made in this paper. To do so implies moving into the more complicated Mie scattering regime, where the wavelength is on the order of the size of the scatterer (tuning thickness). Additionally, we have considered a specific type of reflection coefficient series for which radiative transfer and scattering theory are designed. It remains to be seen what radiative transfer can do for other types of reflection coefficient series, especially for those in which interfaces cannot be grouped into pairs that define scatterers.

Recently, we performed experiments to study multiply scattered Rayleigh waves on a disordered surface (van Wijk et al., 2004). We utilized radiative transfer theory to isolate the effects of scattering and absorption in our laboratory model. Separating these two mechanisms should have applicability in discerning saturated zones sampled by full-waveform well-log data (van Wijk, 2003).

CONCLUSION

Throughout our exploration of the different aspects of radiative transfer, we have made the connection with concepts familiar to seismologists, such as reflection/transmission coefficients, thin beds, and the O'Doherty–Anstey formula. In the process, new features have emerged, such as the diffusion approximation and incoherent wavefield intensity. A quantitative understanding of the incoherent wavefield intensity has important implications for seismology—specifically, for the issue of separating scattering from intrinsic attenuation. In examining the outcomes of radiative transfer theory, our purpose extends beyond promoting the use of this specific theory; we cite radiative transfer as a starting point for the eventual inclusion of multiply scattered waves, especially the incoherent wavefield, into the standard geophysical toolbox used to make inferences about the subsurface.

ACKNOWLEDGMENTS

We thank the scattering-inversion group at the Colorado School of Mines for comments and helpful interaction. In particular, we acknowledge the encouragement of John Scales and the Physical Acoustics Lab. Thanks also go to Ken Larner and Albena Mateeva for helpful reviews of the manuscript. This work was supported by the sponsors of the Consortium Project on Seismic Inverse Methods for Complex Structures at the Center for Wave Phenomena, the National Science Foundation (EAR-0111804 and EAR-0337379), and the Army Research Office (DAAG55-98-1-0277 and DAAD19-03-1-0292).

APPENDIX A

THE GREEN'S FUNCTION FOR THE DIRECTIONAL INTENSITIES

Expressions 11 and 12 show that the 1D radiative transfer equation is actually a system of two partial differential equations in terms of the up- and downgoing intensities. In this paper, we study the sum of the up- and downgoing intensities, or the total intensity, since measuring either the up- or downgoing intensity entails splitting the wavefield into up- and downgoing waves. Such a decomposition requires dense spatial sampling to perform the type of filtering routinely done in vertical seismic profiling (VSP). Here, we solve equations 11 and 12 for the individual up- and downgoing intensities and, as a result, back out the total intensity by summing the 2D intensities.

To begin, we write equations 11 and 12 in matrix form:

$$\frac{\partial \vec{I}}{\partial t} + M\frac{\partial \vec{I}}{\partial z} = N\vec{I} + \vec{S}, \tag{A-1}$$

where

$$\vec{I} = \begin{bmatrix} I_d \\ I_u \end{bmatrix},$$

$$M = \begin{bmatrix} v & 0 \\ 0 & -v \end{bmatrix},$$

$$N = \begin{bmatrix} -\dfrac{B}{\tau_s} - \dfrac{1}{\tau_a} & \dfrac{B}{\tau_s} \\ \dfrac{B}{\tau_s} & -\dfrac{B}{\tau_s} - \dfrac{1}{\tau_a} \end{bmatrix},$$

$$\vec{S} = \begin{bmatrix} S_d \\ S_u \end{bmatrix}. \tag{A-2}$$

We solve the system by Fourier transforming equation A-1 over space, solving the resulting system of ordinary differential equations, and inverse Fourier transforming back to spatial coordinates. With the Fourier conventions

$$\tilde{I}(k) = \frac{1}{2\pi}\int_{-\infty}^{\infty} \vec{I}(z)\exp(ikz)dz,$$

and

$$\vec{I}(z) = \int_{-\infty}^{\infty} \tilde{I}(k) \exp(-ikz) dk \tag{A-3}$$

equation A-1 becomes a system of two ODEs:

$$\frac{\partial \tilde{I}}{\partial t} = (N + ikM)\tilde{I} + \tilde{S}. \tag{A-4}$$

For the source function, we again take a general directional point source with up- and downgoing components S_u and S_d. When we allow the parameter c to govern the directivity of the source as we did previously, the source vector is

$$\vec{S} = \begin{bmatrix} 1+c \\ 1-c \end{bmatrix} \frac{\delta(z)\delta(t)}{2}. \tag{A-5}$$

The solution of the system of ODEs follows that given in standard texts on differential equations (Boyce and DiPrima, 1997). Here, we give the solution in the k-domain:

$$I_d(k,t) = \frac{1}{4\pi} \exp\left(-\frac{Bvt}{\ell_s}\right) \exp\left(-\frac{vt}{\ell_a}\right) \times \left[\left((1-c)\frac{B}{\tau_s} + i(1+c)kv \right) \frac{\sinh\left(t\sqrt{\frac{B^2}{\tau_s^2} - k^2v^2} \right)}{\sqrt{\frac{B^2}{\tau_s^2} - k^2v^2}} + (1+c)\cosh\left(t\sqrt{\frac{B^2}{\tau_s^2} - k^2v^2} \right) \right]. \tag{A-6}$$

$$I_u(k,t) = \frac{1}{4\pi} \exp\left(-\frac{Bvt}{\ell_s}\right) \exp\left(-\frac{vt}{\ell_a}\right) \times \left[\left((1+c)\frac{B}{\tau_s} - i(1-c)kv \right) \frac{\sinh\left(t\sqrt{\frac{B^2}{\tau_s^2} - k^2v^2} \right)}{\sqrt{\frac{B^2}{\tau_s^2} - k^2v^2}} + (1-c)\cosh\left(t\sqrt{\frac{B^2}{\tau_s^2} - k^2v^2} \right) \right]. \tag{A-7}$$

To get the directional intensities in the spatial domain, we must inverse Fourier transform equations A-6 and A-7. Two identities are needed for this inversion:

$$iz \int_{-\infty}^{\infty} \tilde{I}(k) \exp(-ikz) dk = \int_{-\infty}^{\infty} \frac{\partial \tilde{I}(k)}{\partial k} \exp(-ikz) dk \tag{A-8}$$

and, from the theory of Bessel functions (Hemmer, 1961),

$$\int_{-\infty}^{\infty} \cos(kz) \frac{\sin\left(t\sqrt{k^2v^2 - \frac{B^2}{\tau_s^2}} \right)}{\sqrt{k^2v^2 - \frac{B^2}{\tau_s^2}}} dk = \frac{\pi}{v} I_0\left[\frac{B}{\ell_s}\sqrt{v^2t^2 - z^2} \right] H(vt - |z|), \tag{A-9}$$

where I_0 is the modified Bessel function of zeroth order and H is the Heaviside step function.

After inverting the Fourier transform, we obtain for the downgoing intensity

$$I_d(z,t) = \frac{1}{4}\exp\left(-\frac{Bvt}{\ell_s}\right)\exp\left(-\frac{vt}{\ell_a}\right)\left[2(1+c)\delta(vt-z) + \frac{B}{\ell_s}H(vt-|z|)\left[(1-c)I_0\left(\frac{B}{\ell_s}\sqrt{v^2t^2 - z^2} \right) + (1+c)\sqrt{\frac{vt+z}{vt-z}} I_1\left(\frac{B}{\ell_s}\sqrt{v^2t^2 - z^2} \right) \right] \right] \tag{A-10}$$

and, for the upgoing intensity,

$$I_u(z,t) = \frac{1}{4}\exp\left(-\frac{Bvt}{\ell_s}\right)\exp\left(-\frac{vt}{\ell_a}\right)\left[2(1-c)\delta(vt+z) + \frac{B}{\ell_s}H(vt-|z|)\left[(1+c)I_0\left(\frac{B}{\ell_s}\sqrt{v^2t^2 - z^2} \right) + (1-c)\sqrt{\frac{vt-z}{vt+z}} I_1\left(\frac{B}{\ell_s}\sqrt{v^2t^2 - z^2} \right) \right] \right], \tag{A-11}$$

where I_1 is the modified Bessel function of the first order. The modified Bessel functions I_0 and I_1 should not be confused with the symbols used for the various intensities (I_t, I_d, I_u, and I_n). Equations A-10 and A-11 show that the two modified Bessel functions that make up the incoherent intensity are sensitive to different aspects of the source radiation pattern. For instance, if the source were unidirectional ($c = -1$ or $c = 1$), the zeroth-order modified Bessel function would come from one direction and the first-order modified Bessel from the other. In the absence of phase information, perhaps the directional intensities can yield information about spatial variations in the material properties. Adding equations A-10

and A-11 gives the total intensity:

$$I_t(z,t) = \frac{1}{2}\exp\left(-\frac{Bvt}{\ell_s}\exp\frac{vt}{\ell_a}\right)\left[(1-c)\delta(vt+z) + (1+c)\delta(vt-z) + \frac{B}{\ell_s}H(vt-|z|)\right] \times \left[I_0\left(\frac{B}{\ell_s}\sqrt{v^2t^2-z^2}\right) + \frac{vt+cz}{\sqrt{v^2t^2-z^2}} \times I_1\left(\frac{B}{\ell_s}\sqrt{v^2t^2-z^2}\right)\right]\right]. \quad \text{(A-12)}$$

The result by Hemmer (1961) is obtained from equation A-12 for the case of an isotropic source ($c = 0$) and isotropic scattering ($B = 1/2$).

APPENDIX B

THE SCATTERING CROSS-SECTION IN THE LIMIT OF WEAK SCATTERING

The scattering cross-section for a thin bed is (Sheng, 1995)

$$\sigma_s(k_0) = \frac{1}{2}k_0^2h^2\left[1-\left(\frac{v}{v_0}\right)^2\right]^2, \quad \text{(B-1)}$$

where k_0 is the wavenumber in the background medium, h is the thickness of the thin bed, v is the velocity of the thin bed, and v_0 is the velocity of the background medium. The k_0^2 dependence of σ_s is the hallmark of Rayleigh scattering in one dimension. Equation B-1 is the first term of a power series in k_0h and can be derived from the 1D scalar wave equation by requiring that the displacement and its spatial derivative be continuous at both boundaries of a 1D scatterer, or thin bed. These same boundary conditions at an interface yield the reflection and transmission coefficients:

$$R = \frac{v-v_0}{v+v_0} \quad \text{and} \quad T = \frac{2v}{v+v_0}. \quad \text{(B-2)}$$

These reflection and transmission coefficients for scalar waves are equivalent to those for constant-density acoustic media.

Assume that the velocity of the thin bed can be expressed as $v = v_0\,(1+\alpha)$, with $\alpha \ll 1$. This is the case of a small reflection coefficient. For an assemblage of thin beds with varying velocities, α represents the rms perturbation from the background velocity. Substituting this relation for v into equation B-1 gives

$$\sigma_s(k_0) = \frac{1}{2}k_0^2h^2[1-(1+\alpha)^2]^2. \quad \text{(B-3)}$$

Keeping the lowest order term in α,

$$\sigma_s(k_0) \approx 2k_0^2h^2\alpha^2. \quad \text{(B-4)}$$

To satisfy equation 16, we need to show that the scattering cross-section in the weak scattering limit, equation B-4, is equal to $8k_0{}^2h^2R^2$. From equation B-2,

$$8k_0^2h^2R^2 = 8k_0^2h^2\left(\frac{v-v_0}{v+v_0}\right)^2. \quad \text{(B-5)}$$

Substituting $v = v_0(1+\alpha)$ into equation B-5 gives

$$8k_0^2h^2R^2 = 8k_0^2h^2\left(\frac{\alpha}{2+\alpha}\right)^2. \quad \text{(B-6)}$$

Again, keeping the lowest order term in α, we obtain that the right-hand side of equation B-6 equals $2k_0^2h^2\alpha^2$, identical to equation B-4. Hence, in the weak scattering limit for thin beds, $8k_0^2h^2R^2 = \sigma_s$.

APPENDIX C

DETAILS ON THE NUMERICAL SIMULATIONS

Our numerical approach uses the centered-difference approximation to the second spatial and temporal derivatives in the 1D scalar wave equation:

$$\frac{u(z,t+\Delta t) - 2u(z,t) + u(z,t-\Delta t)}{\Delta t^2} = v^2(z)\frac{u(z+h,t) - 2u(z,t) + u(z-h,t)}{h^2} + S(z,t), \quad \text{(C-1)}$$

where $u(z, t)$ is the displacement field as a function of depth and time, Δt is the time increment, h is the spatial discretization length, $v(z)$ is the background velocity, and $S(z, t)$ is the source. Performing a harmonic analysis of the above difference equation yields both the dispersion and stability properties of our numerical scheme (Alterman and Loewenthal, 1970). The resulting stability condition requires that

$$v(z)\Delta t \le h. \quad \text{(C-2)}$$

In addition, the numerical dispersion relation can be expressed as

$$\cos\omega\Delta t = 1 - \frac{2\Delta t^2v^2(z)}{h^2}\sin^2\left(\frac{kh}{2}\right), \quad \text{(C-3)}$$

where ω is the angular frequency and k is the wavenumber. If $\omega\Delta t$ and kh are small parameters ($\ll 1$), equation C-3 simplifies to $\omega^2 = v^2(z)\,k^2$. In other words, the numerical dispersion vanishes as the waves are better sampled in time and space. For our simulations, we set the number of gridpoints per dominant wavelength to 30, ensuring that numerical dispersion posed no problem.

We have equipped the finite-difference stencil of equation C-1 with absorbing boundary conditions at the edges of the numerical grid. For this simple 1D case, Clayton–Enquist boundary conditions (or radiation boundary conditions) can be constructed that perfectly absorb any outgoing waves (Clayton and Enquist, 1977). In higher dimensions, this approach fails and other techniques, most notably the perfectly matched layer (PML) method, must be used (Chew and Liu, 1996). When we take the numerical domain to extend from $z = -\alpha$ to $z = L + \alpha$, a discrete one-way wave equation at the boundary $z = -\alpha$ is

$$\frac{u(-\alpha,t) - u(-\alpha,t-\Delta t)}{\Delta t} = v\frac{u(-\alpha+h,t-\Delta t) - u(-\alpha,t-\Delta t)}{h}. \quad \text{(C-4)}$$

We require that the velocity be constant, $v(z) = v$, for the boundary point and the nearest interior gridpoint. Equation C-4 can be rearranged to solve for $u(-\alpha, t)$, the displacement on the boundary, as a function of the displacement at the boundary at the previous time step, $u(-\alpha, t-\Delta t)$, and the displacement at the nearest interior gridpoint at the previous time step, $u(-\alpha + h, t - \Delta t)$. Hence, the absorbing boundary condition is explicit in time.

Because of the approximation of the derivatives in equation C-4, the boundary condition does not perfectly absorb in general. Interpolation errors arising from the approximate derivatives cause sizable reflections from the boundary. The exception is when $v\Delta t/h = 1$. In that case, the absorbing boundary condition becomes

$$u(-\alpha, t) = u(-\alpha + h, t - \Delta t). \qquad \text{(C-5)}$$

This boundary condition assigns the value of displacement at the nearest gridpoint from the previous time step to the boundary point, $u(-\alpha, t)$, thereby mimicking 1D propagation when the time step, grid spacing, and velocity are chosen to obey $h/\Delta\, t = v$. In other words, for this choice, there are no interpolation errors. From equation C-2, this combination corresponds to the equality and still allows for a stable numerical scheme.

REFERENCES

Aki, K., and P. Richards, 1980, Quantitative seismology: W. H. Freeman Company.

Alterman, Z. S., and D. Loewenthal, 1970, Seismic waves in a quarter and three-quarter plane: Geophysical Journal of the Royal Astronomical Society, **20**, 101–126.

Banik, N. C., I. Lerche, and R. T. Shuey, 1985, Stratigraphic filtering—Part I: Derivation of the O'Doherty-Anstey formula: Geophysics, **50**, 2768–2774.

Bleistein, N., J. K. Cohen, and J. W. Stockwell, Jr., 2001, Mathematics of multidimensional seismic imaging, migration, and inversion: Springer-Verlag, New York.

Boas, D. A., L. E. Campbell, and A. G. Yodh, 1995, Scattering and imaging with diffusing temporal field correlations: Physical Review Letters, **75**, 1855–1858.

Boore, D. M., 1970, Finite-difference solutions to the equations of elastic wave propagation, with applications to Love waves over dipping interfaces: Ph.D. dissertation, Massachusetts Institute of Technology.

Boyce, D. M., and R. C. DiPrima, 1997, Elementary differential equations: John Wiley & Sons, Inc.

Chandrasekhar, S., 1960, Radiative transfer: Dover Publications, Inc.

Chew, W. C., and Q. H. Liu, 1996, Perfectly matched layers for elastodynamics: A new absorbing boundary condition: Journal of Computational Acoustics, **4**, 341–359.

Clayton, R., and B. Enquist, 1977, Absorbing boundary conditions for acoustic and elastic wave equations: Bulletin of the Seismic Society of America, **67**, 1529–1540.

Feynman, R. P., R. B. Leighton, and M. Sands, 1963, The Feynman lectures on physics: Addison-Wesley Publishing Company.

Goedecke, G. H., 1977, Radiative transfer in closely packed media: Journal of the Optical Society of America, **67**, 1339–1348.

Hemmer, P. C., 1961, On a generalization of Smoluchowski's diffusion equation: Physica A, **27**, 79–82.

Hendrich, A., A. S. Martinez, R. Maynard, and B. A. van Tiggelen, 1994, The role of the step length distribution in wave-diffusion: Physics Letters A, **185**, 110–112.

Hennino, R., N. Trégourès, N. M. Shapiro, L. Margerin, M. Campillo, B. A. van Tiggelen, and R. L. Weaver, 2001, Observation of equipartition of seismic waves: Physical Review Letters, **86**, 3447–3450.

Ishimaru, A., 1997, Wave propagation and scattering in random media: Oxford University Press.

Lax, M., 1951, Multiple scattering of waves: Reviews of Modern Physics, **23**, 287–310.

Lindley, David, 2001, Boltzmann's atom: The Free Press.

Margerin, L., M. Campillo, N. M. Shapiro, and B. A. van Tiggelen, 1999, Residence time of diffusive waves in the crust as a physical interpretation of coda Q: Application to seismograms recorded in Mexico: Geophysical Journal International, **138**, 343–352.

Morse, P., and H. Feshbach, 1953, Methods of theoretical physics: McGraw-Hill Book Company.

O'Doherty, R. F., and N. A. Anstey, 1970, Reflections on amplitudes: Geophysical Prospecting, **19**, 430–458.

Paasschens, J. C., 1997, Solution of the time-dependent Boltzmann equation: Physical Review E, **56**, 1135–1140.

Papanicolaou, G., 1998, Mathematical problems in geophysical wave propagation: Documenta Mathematica, Extra Volume ICM, 1–25.

Resnick, J. R., I. Lerche, and R. T. Shuey, 1986, Reflection, transmission and the generalized primary wave: Geophysical Journal of the Royal Astronomical Society, **87**, 349–377.

Saaty, Thomas L., 1981, Modern nonlinear equations: Dover.

Sato, H., and M. C. Fehler, 1998, Seismic wave propagation and scattering in the heterogeneous earth: Springer-Verlag, New York.

Scales, J. A., and K. van Wijk, 2001, Tunable multiple-scattering system: Applied Physics Letters, **79**, 2294–2296.

Scheffold, F., R. Lenke, R. Tweer, and G. Maret, 1999, Localization or classical diffusion of light?: Nature, **398**, 206–207.

Schuster, A., 1905, Radiation through a foggy atmosphere: Journal of Astrophysics, **21**, 1–22

Shapiro, S., and P. Hubral, 1999, Elastic waves in random media: Springer Publishing Company, Inc.

Shapiro, S., and H. Zien, 1993, The O'Doherty-Anstey formula and localization of seismic waves: Geophysics, **58**, 736–740.

Sheng, P., 1995, Introduction to wave scattering, localization, and mesoscopic phenomena: Academic Press.

Spencer, T. W., J. R. Sonnad, and T. M. Butler, 1982, Seismic Q—Stratigraphy or dissipation: Geophysics, **47**, 16–24.

Turner, J., 1994, Radiative transfer of ultrasound: Ph.D. thesis, University of Illinois.

van Tiggelen, B. A., A. Lagendijk, A. Tip, and G. F. Reiter, 1991, Effect of resonant scattering on localization of waves: Europhysics Letters, **15**, 535–540.

van Wijk, K., 2003, Multiple scattering of surface waves: Ph.D. dissertation, Colorado School of Mines.

van Wijk, K., M. Haney, and J. A. Scales, 2004, 1D energy transport in a strongly scattering laboratory model: Physical Review E, **69**, 036611.

Wiersma, D. S., P. Bartolini, A. Lagendijk, and R. Righini, 1997, Localization of light in a disordered medium: Nature, **390**, 671–673.

Wu, R. S., 1993, Separation of scattering and absorption in 1-D random media from spatio-temporal distribution of seismic energy: 63rd Ann. Internat. Mtg. Soc. Expl. Geophys. Expanded Abstracts, 1014–1017

——— 1998, Spatio-temporal distribution of seismic power for a random absorptive slab in a half space, *in* G. Papanicolaou, Ed., Wave propagation in complex media: Springer Publishing Inc., 273–287.

Wu, R. S., and K. Aki, 1988, Multiple scattering and energy transfer of seismic waves—Separation of scattering effect from intrinsic attenuation II: Application of the theory to Hindu Kush region: Pure and Applied Geophysics, **128**, 49–80.

Wu, R. S., and X. B. Xie, 1994, Separation of scattering and absorption in 1-D random media II: Numerical experiments on stationary problems: 64th Annual International Meeting, SEG, Expanded Abstracts, 1302–1305.

Zauderer, E., 1989, Partial differential equations of applied mathematics: Wiley Interscience.